Influence of Stress Concentrator Shape and Testing Temperature on Impact Bending Fracture of 17Mn1Si Pipe Steel

S.V. Panin[1,2], I.V. Vlasov[1,2], P.O. Maruschak[3], D.D. Moiseenko[1], F. Berto[4] and A. Vinogradov[4]

[1]Institute of Strength Physics and Materials Science SB RAS, 2/4, pr. Akademicheskii, Tomsk, 634055, Russia

[2]Ternopil Ivan Pul'uj National Technical University, 56, Ruska str. Ternopil, 46001, Ukraine

[3]National Research Tomsk Polytechnic University, 30, Lenin Avenue, Tomsk, 634050, Russia

[4]Norwegian University of Science and Technology, Richard Birkelands vei 2b, 7491 Trondheim, Norway

INTRODUCTION

A common tendency in transportation pipeline development, particularly, for main gas and oil pipelines, is a gradual increase in their service life and performance [1]. The problem is particularly acute since the pipelines often operate in unfavorable weather conditions, e.g., at low temperatures. A challenging task in this respect is to extend the service life of pipe steels by improving their mechanical properties [2]. Specifically, the fracture toughness – the major characteristics of crack resistance - has to be increased.

Main detrimental factors affecting the strength and crack resistance of pipe steels are attributed to tensile stresses and corrosion of the outer surface of pipes arising in underground conditions due to delamination or rupture of protective coating and localized corrosion of the inner surface [3].

Currently available approaches to characterizing the base metal ductility allow estimating the dynamic crack initiation conditions that are crucial for the prevention of gas and oil pipeline failure [4]. It requires development of robust methods for the fracture energy determination in pipe steels with account of the shape of stress concentrators. These data can be used to account for the influence of embrittlement factors on the impact deformation resistance of pipe steels. Furthermore, modern low-carbon steels produced by thermomechanical processing of the initial sheet have different sensitivity to the concentrator shape and temperature/force loading parameters. It is therefore important to understand the fracture mechanisms operating at different stress stiffness values.

The present paper is aimed at obtain a deeper insight into the influence of the notch shape on the impact fracture of 17Mn1Si steel at different temperatures with a focus on the low temperature fracture behavior.

EXPERIMENTAL

A batch of specimens 10 × 10 × 55 mm with *V*-, *U*- and *I*-shaped notches of equal depth (2 mm) was machined. *V*- and *U*-notches were introduced by standard milling cutters (ASTM E 23); *I*-notches were made by electroerosion. Notch tip radius: *U*-1.0 mm; *V*-0.25 mm; *I*-0.1 mm. Before low-temperature impact testing, the specimens were kept in a cooling chamber Lauda rp870 for 10 minutes in the temperature range from –60 ºC to 0 ºC. They were then rapidly mounted (did not exceed 5 seconds) into the grips of the impact pendulum Instron 450MPX for testing. At least three specimens of each type were tested at temperatures 20, 0, –20, –40 and –60 ºC, Table 1.

INVESTIGATION RESULTS

Typically for structural steels, the test temperature dependence of impact toughness (Fig. 1a) exhibits several characteristics regions [5, 6]. In the lower shelf (from *T* = –60 ºC to *T* = –40 ºC) the specimen exhibits a fracture without pronounced signs of plastic deformation. The increase of the test temperature up to about –20 ºC results in a combined brittle and ductile fracture mechanisms. The upper shelf (from –0 ºC to 20 ºC) corresponds to the region of ductile fracture characterized by intensive plastic deformation on both micro- and macroscale. It is commonly accepted [6, 7], that fracture in each region is mediated by specific microscopic mechanisms [8].

It should be noted that the impact toughness of *U*-notched specimens is about 3 times higher in the entire test temperature range than that of *V*-notched specimens (Fig. 1). It can be assumed approximately that the impact toughness value for specimens with all three types of notches linearly decreases with the decreasing test temperature.

The obtained dynamic loading curves of the specimens corroborate their sensitivity to changes in the macrofracture localization conditions which are associated with the notch shape (Fig. 1). The loading curve shape is typical of ductile fracture within the entire studied temperature range from 20 °C to –60 °C [9] for all specimens tested including those with sharper *V*- and *I*-notches. The shape of the impact diagrams of the *V*- and *I*-notched specimens is almost the same, which indicates that crack initiation and growth occur similarly.

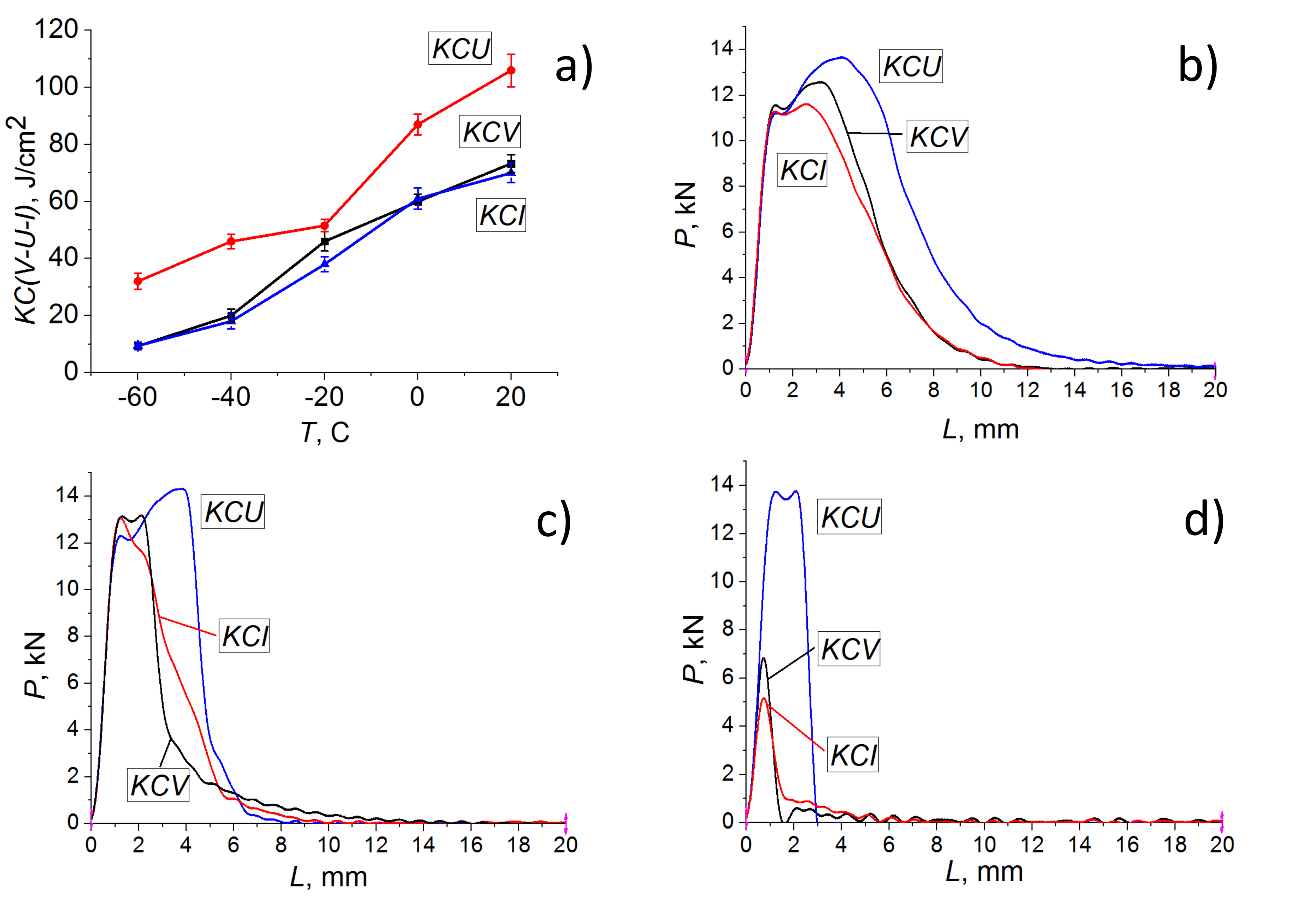

Fig. 1. Temperature dependence of impact toughness (a); impact diagrams in the load/displacement coordinates at test temperatures: 20 ºC (b); -20 ºC (c); –60 ºC (d); for *V*-, *U*-, and *I*-notched specimens.

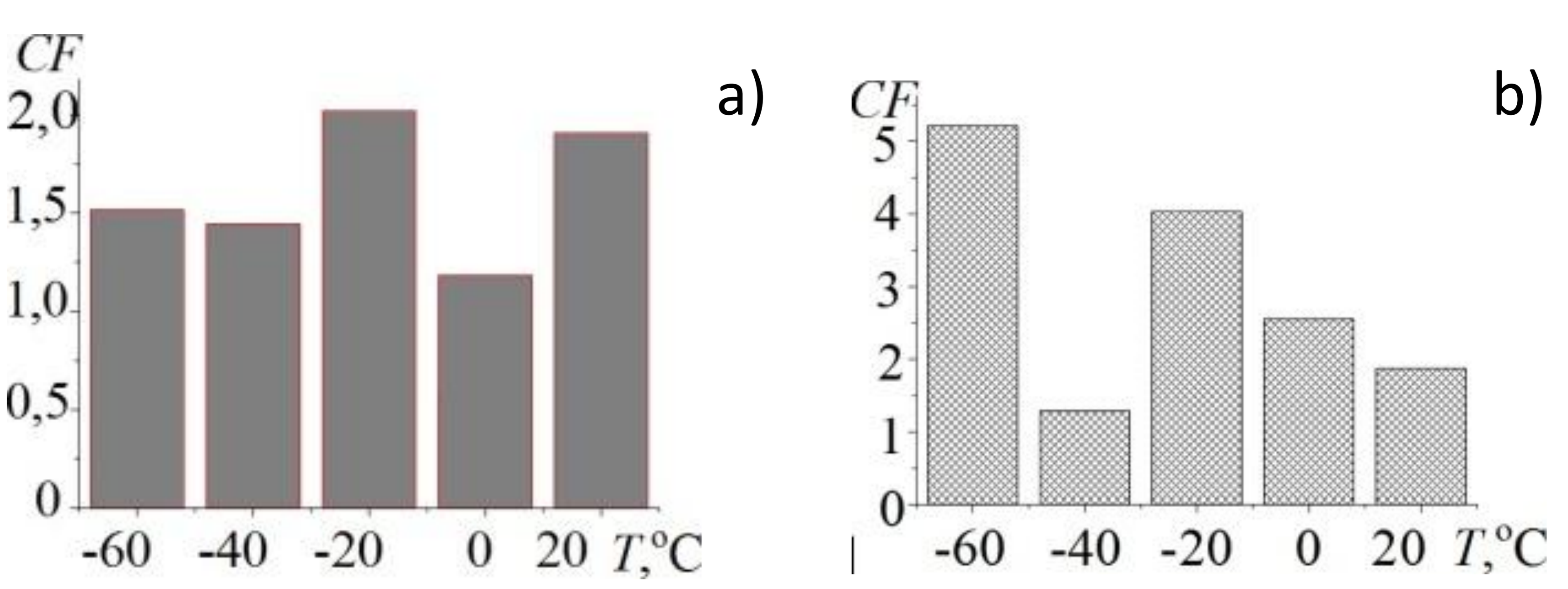

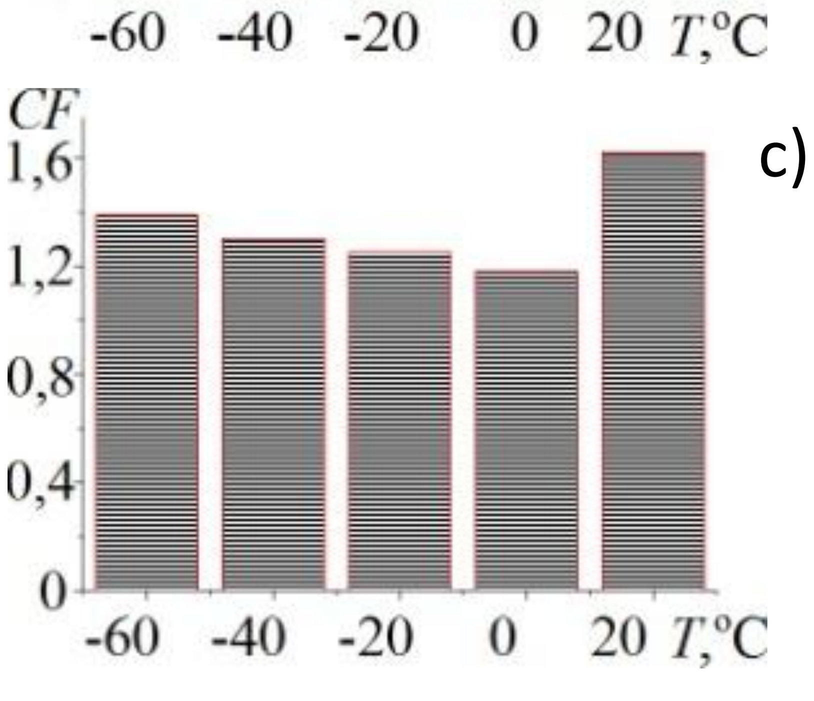

Fig. 2. Temperature dependence of the *CF* parameter for 17Mn1Si steel specimens with *V*- (a), *U*- (b), *I*-notches (c).

Table 1. Impact toughness test results and fracture energy of 17Mn1Si steel specimens with different notches under impact bending (*i* – initiation, *p* – propagation)

T, ºC	Impact toughness (*KCV-U-I*, J/cm²) and Fracture energy, (*A*, J)											
	V-notch				*U*-notch				*I*-notch			
	KCV	A_t	A_i	A_p	*KCU*	A_t	A_i	A_p	"*KCI*"	A_t	A_i	A_p
–60	9.3±1.1	7.26	2.47	4.79	32±2.8	25.02	20.22	4.80	9.4±1.3	7.35	2.06	5.29
–40	20±2.3	15.82	4.86	10.96	46±2.5	35.53	7.91	27.62	18±2.7	14.47	3.36	11.11
–20	46±3.4	36.27	18.31	17.96	51.6±2.2	51.55	38.76	12.79	38±2.6	37.98	7.65	30.33
0	60±2.6	47.11	7.25	39.86	87±3.9	68.39	41.59	26.80	61±3.7	48.01	7.39	40.62
20	73±3.2	57.51	27.37	30.14	106±5.7	80.75	37.55	43.20	70±3.4	55.15	21.13	34.02

***V*-notch.** The specimens of 17Mn1Si steel fracture in a ductile manner at test temperatures from 20 ºC to –20 ºC, which is evidenced by gradually ascending and descending parts of the loading curve (Fig. 1b,c, curve *KCV*). The microscale deformation mechanisms result in effective stress relaxation [10]. At –40 ºC and –60 ºC the fracture diagrams narrows and peaks. The shape of the descending curve part points to brittle crack propagation [10]. This is especially typical of the test temperature *T* = –60 ºC at which the maximum load decreases down to P_{max} = 7 kN, which is indicative of a partial loss of the bearing capacity of the material [11].

***I*-notch.** The shape of the loading diagram (Fig. 1, curve *KCI*) is similar to that of the specimen with the *V*-shaped concentrator. In our opinion, this is due to the fact that plastic deformation ahead the tip of the main crack gives rise to partial stress relaxation during crack propagation in the studied steel. At *T* = –60 ºC, the maximum load value decreases even more abruptly down to P_{max}=5 kN. This is testimony to a more pronounced embrittlement effect of the stress concentrator, which corresponds well to the minimum notch tip radius.

***U*-notch.** The impact fracture of notched 17Mn1Si steel specimens with the maximum notch tip radius is accompanied by considerable plastic deformation. The observed macroscopic deformation behavior of the material bears witness to the activation of relaxation processes, which leads to an increase in the height and width of the impact diagram in the entire studied temperature range (Fig. 1b). Thus, an increase in the material volume involved in deformation resistance, like for the *U*-notch due to its larger radius, increases resistance to macrocrack initiation and growth. However, this occurs at lower values of load *P* on the stage of elastic deformation as compared to the case of the *I*-shaped notch.

The yield plateau in the impact diagrams of *I*-notched specimens is only slightly seen. This is indicative of local hardening processes on early deformation stages, which are accompanied by a decrease in the resistance of steel to strain localization in bending (which is quite undesirable for pipelines).

Additionally, as is known, the total fracture energy of Charpy specimens (A_t) consists of two main parts: crack initiation energy (A_i), and crack propagation energy (A_p) (Table 1). Hashemi [5] suggested that in the presence of an in-service defect the most important characteristic reflecting the material capability to the propagation of such defects was the crack propagation energy. Thus, he proposed the following fracture parameter:

$$CF = \frac{A_t}{(A_t - A_i)}$$

Results of *CF* estimation, calculated from Eq. (1) for specimens with differently shaped notches within the studied test temperature range are shown in Fig. 2. The results demonstrate that 17Mn1Si steel has significant ductility in the case of a sharp crack-like notch. In view of Hashemi's physical interpretation [5], the minimum *CF* value indicates that the least energy is needed for pipeline fracture arrest in the presence of a sharp crack-like notch.

It should be noted that the use of the *CF* parameter is pertinent in the presence of a large sharp defect in the pipe, or for pipes under long-term operation conditions. Considering the steel in the as-supplied state, the present results show that the material has sufficient ductility. However, the *CF* parameter of steel decreases during operation. The impact toughness values of 17Mn1Si steel determined by taking into account the total fracture energy of Charpy specimens are given in Table 1. In the way of discussion, the authors would like to highlight a few features in the data. Firstly, the energy for crack initiation at *T*=-40 ºC has dropped significantly while the energy for crack propagation increased. Secondly, the same is true for the *V*-shaped notch specimen fractured under impact bending at *T*=0 ºC. Thirdly, the values of the fracture energy for the *I*-notched specimen being tested at ambient temperature also appeared different from expectations.

The mentioned "variations" are most probably related to the influence of the testing temperature as well as of the stress-strain state in the loaded specimens. From the microscale fracture mechanism point of view, it should be underlined that irreversible deformations under quasi-brittle fracture are rather low while fracture energy is predominantly determined the by the stress stiffness parameters. Under ductile failure, the decisive role is related to accumulated plastic strains [12, 13]. The experimental data presented in Tables 1 highlight the fact that the fracture energy in the brittle-to-ductile transition regime is fundamentally influenced by the stress stiffness.

CONCLUSION

An approach towards fracture characterization has been suggested based on the description of elastic-plastic deformation of impact loaded specimens on the stage of crack initiation and growth at ambient and lower temperatures. The analysis of the shape of impact loading diagrams and energy fracture values for impact loaded specimens of pipe 17Mn1Si steel revealed the fracture mechanisms of this steel depending on the notch shape.

It was found that the test temperature reduction plays the decisive role in plastic strain localization and subsequent impact fracture of specimens with different-shaped notches. This is reflected in localization of deformation processes and decrease in crack propagation energy.

ACKNOWLEDGMENTS

The work was performed in the framework of fundamental research projects of the Russian State Academies of Sciences (2013–2020), with a partial support of RFBR Grant No. 15-08-05818_a, and Project of the Headquarter of the Russian Academy of Sciences on Artic research. The impact tests were carried out at Tomsk Polytechnic University within the framework of Tomsk Polytechnic University Competitiveness Enhancement Program grant.

REFERENCES

1. S.H. Hashemi, International Journal of Pressure Vessels and Piping **85**, 879-884 (2008).
2. A.B. Arabei, I.Yu. Pyshmintsev, V.M. Farber, et. al., Steel in Translation **42**, 212-218 (2012).
3. M. Ben Amara, G. Pluvinage , J. Capelle, Z. Azari, Physical Mesomechanics **8**, 355-369 (2015).
4. P.E. O'Donoghue, M.F. Kanninen, C.P. Leung, G. Demofonti, S. Venzi, International Journal of Pressure Vessels and Piping **70**, 11-25 (1997).
5. S.H. Hashemi, International Journal of Pressure Vessels and Piping **86(8)**, 533-540 (2009).
6. S.A. Kotrechko, Yu. Ya. Meshkov, Strength of Materials, **33(4)**, 356-361 (2001).
7. S.H. Hashemi, D. Mohammadyani, M. Pouranvari, S.M. Mousavizadeh, Fatigue & Fracture of Engineering Materials & Structures **32**, 33–40 (2009).
8. V.E. Panin, V.E. Egorushkin, A.V. Panin, A.G. Chernyavskii, Phys. Mesomech., **19 (3)** 255-268 (2016).
9. P.K.C. Venkatsurya, R.D. K. Misra, M.D. Mulholland, M. Manohar, J.E. Hartmann, Metallurgical and Materials Transactions A **45(5)**, 2335–2342 (2014).
10. P.O. Maruschak, I.M. Danyliuk, R.T. Bishchak, T. Vuherer, Central European Journal of Engineering **4**, 408–415 (2014).
11. G.C. Sih, D.Y. Tzou, Theoretical and Applied Fracture Mechanics **5**, 189-203 (1986).
12. P.O. Marushchak, R.T. Bishchak, B. Gliha, A.P. Sorochak, Materials Science **46**, 568–572 (2011).
13. P.V. Yasnii, Yu.I. Pyndus, V.B. Glad'o, I.B. Okipnyi, I.V. Shul'gan, Strength of Materials **43**, 113-121 (2011).